

Universal Conductance Fluctuations in Metals

P. A. Lee

Physics Department, Massachusetts Institute of Technology, Cambridge, Massachusetts 02139

and

A. Douglas Stone^(a)

IBM T. J. Watson Research Center, Yorktown Heights, New York 10598

(Received 1 July 1985)

The conductance of any metallic sample is predicted to fluctuate as a function of chemical potential or magnetic field by an amount of order e^2/h ($\approx 4 \times 10^{-5} \Omega^{-1}$) independent of sample size and degree of disorder as long as the temperature is low enough so that kT and the inelastic-scattering rate are less than the inverse time to diffuse across the sample. The theory is shown to be in excellent agreement with numerical simulations and explains many features of experiments on small wires and rings.

PACS numbers: 72.15.-v, 72.20.My

Recent experimental studies¹ of resistance in small metallic wires and rings (typical dimensions $400 \times 400 \times 8000 \text{ \AA}^3$) at low temperatures have uncovered unexpected fluctuations (typically 1 part in 10^3) as a function of magnetic field. Numerical simulations by Stone² have reproduced many of the observed features, making it clear that the fluctuations are a consequence of quantum interference when the inelastic diffusion length exceeds sample dimensions. However, it remains unclear how the 10% fluctuations found in simulations of relatively small samples should be extrapolated to the experimental situation. Since the experiments and simulations are all performed in the highly conducting diffusive regime, $k_F l \gg 1$ (l is the mean free path), it is possible to treat the problem by use of weak-scattering diagrammatic techniques. Here we report the results of such a calculation which show that conductance fluctuations of the order of e^2/h are a universal feature of quantum transport in the low-temperature limit. In particular, they are independent of both the degree of disorder and the sample

size at zero temperature. This simple result is consistent with both experiments and simulations, showing that the experiments actually revealed something fundamental about quantum transport, rather than simply "finite-size effects."

We consider the conductance of noninteracting electrons in the following system: a finite disordered region of volume $V = L_x^{d-1} L_z$, extended to $\pm \infty$ in the z direction by the attachment of ideal "leads," with an electromagnetic field applied only to the disordered region. The transport of electrons through the disordered region can be considered as a scattering problem where electrons from the leads are transmitted or reflected by the random potential. It was shown³ that the Kubo formula for the conductance of such a system (in units of e^2/h , including spin) is equivalent to $g = 2 \text{Tr}(t^T t)$, where t is the transmission matrix. This expression for g should be valid for $L_z \gg l$, the regime of interest.

The quantity that we calculate is the correlation function

$$F(\Delta E, \Delta B) = \langle g(E_F, B) g(E_F + \Delta E, B + \Delta B) \rangle - \langle g(E_F, B) \rangle^2, \quad (1)$$

where the angular brackets denote the ensemble average. Our hypothesis is that the dependence of g on B and E for a given sample is effectively random, so that the correlation function will decay to zero over some range in ΔE and ΔB . Then an ensemble average at fixed E , ΔE , B , and ΔB is equivalent to an average over many values of E and B at fixed ΔE and ΔB . Thus the quantities we calculate can be directly compared with experiment in a single sample: $F(\Delta E, \Delta B)$ in metal-oxide-semiconductor field-effect transistors and $F(\Delta E = 0, \Delta B)$ in any metallic system.

In an exact eigenstate representation $F(\Delta E, \Delta B)$ involves the impurity average of a product of eight wave functions. The wave functions experience the same impurity potential and it is known that on the average wave functions nearby in energy are correlated in

space.^{4,5} Such correlations are the consequence of quantum diffusion. To evaluate the impurity average, we write F in terms of Green's functions. A diagrammatic representation of g (based on Ref. 3) is shown in Fig. 1(a), where the unaveraged Green's function propagates from r_1 to r_1' and back and is scattered by impurities at r_2, \dots, r_n , and each segment can be either advanced or retarded Green's functions, G^\pm . To calculate F we draw two such loops with the outer and inner loop representing electrons with Fermi energies E_F and $E_F + \Delta E$ and in fields B and $B + \Delta B$, respectively. Upon impurity averaging only those diagrams in which the impurity scattering connects the two loops contribute to F . The most singular diagrams [shown in Figs. 1(b)–1(f)] are generated by our start-

ing with two loops with self-energy correction due to impurity scattering, connecting them with impurity ladders, and inserting four current vertices in all possible ways.

To see the general structure of the divergences in this theory, let us consider an infinite system with $\Delta B = 0$. The diagrams can be evaluated in momentum space, and at $T = 0$ each impurity ladder in Fig. 1 gives rise to a diffusion pole $(\tau D q^2 - i \Delta E \tau)^{-1}$ and all the poles occur with the same q and ΔE . The q integration is then seen to be infrared divergent below four dimensions as q_c^{d-4} , where $q_c \approx L^{-1}$ is a finite-size cutoff. This infrared divergence is the origin of the strong conductance fluctuations which do not decrease with increasing sample size. To see this, note that the

standard semiclassical assumptions would imply $\text{rms}(g)/g \sim 1/(L^d)^{1/2}$ {where $\text{rms}(g) = [\text{var}(g)]^{1/2}$ }. In the metallic regime g is proportional to L^{d-2} , so that we would have $\text{var}(g) \sim L^{d-4}$. The factors $q_c^{d-4} \sim L^{4-d}$ arising from the infrared divergences exactly cancel all the size dependence in $\text{var}(g)$. The existence of this kind of divergence was first pointed out by Maldague.⁵

To evaluate Eq. (1) for a finite sample the diagrams must be formulated in real space. Consider Fig. 1(b); because the averaged Green's function \bar{G} is short ranged, the portion of the diagram connected to the current vertices yields a constant. The rest of the diagram is proportional to

$$\int_V d^3r \int_V d^3r' P(\mathbf{r}, \mathbf{r}', \Delta E, \Delta B) P(\mathbf{r}, \mathbf{r}', \pm \Delta E, \Delta B),$$

where $\pm \Delta E$ refers to the choice of G^\pm in Fig. 1(b) and P is the diffusion propagator representing the sum of the ladder diagrams. P satisfies the diffusion equation⁶

$$[-i\Delta E + D(-i\nabla + e\Delta\mathbf{A})^2 + \tau_{\text{in}}^{-1}]P(\mathbf{r}, \mathbf{r}', \Delta E, \Delta B) = \tau^{-1}\delta(\mathbf{r} - \mathbf{r}'), \tag{2}$$

where τ is the elastic-scattering time and $\Delta\mathbf{A}$ is the vector potential corresponding to the difference field $\Delta\mathbf{B}$. The magnetic field has been treated within the semiclassical approximation,⁶ where its effect is simply to multiply $\bar{G}(\mathbf{r} - \mathbf{r}')$ by the phase factor $\exp(ie \int_{\mathbf{r}'}^{\mathbf{r}} \mathbf{A} \cdot d\mathbf{s})$. Normally such phase factors will then cancel in

the particle-hole channel, but in this case the particle and hole experience different fields and acquire a phase difference which leads to the appearance of $\Delta\mathbf{A}$ in Eq. (2).

In Eq. (2) we have inserted by hand an inelastic-scattering rate τ_{in}^{-1} which may be due to electron-electron or electron-phonon collisions at finite temperature. We note that usually such a term in the diffusion equation is forbidden by particle conservation; however, in the present problem, because the two loops in Figs. 1(b)–1(f) refer to two different measurements, they are connected only by impurity averaging and not interaction lines, and the usual cancellation between self-energy and vertex corrections does not occur.

A useful spectral representation of the solution of Eq. (2) is $P(\mathbf{r}, \mathbf{r}') = \sum_\mu \phi_\mu^*(\mathbf{r}) \phi_\mu(\mathbf{r}') / \lambda_\mu$, where the ϕ_μ and λ_μ are the eigenvectors and eigenvalues (subject to the appropriate boundary conditions) of the equation $\hat{R} \phi_\mu = \lambda_\mu \phi_\mu$ and \hat{R} is the differential operator appearing in Eq. (2). Then the double integral for diagram 1(b) becomes $\sum_\mu \lambda_\mu^{-2}$. The boundary conditions⁷ are determined by the physical requirement that we have coupling to ideal "leads" in the current direction and perfectly reflecting walls in the transverse directions. This implies that $\partial P / \partial x = \partial P / \partial y = 0$ at the walls, and $P = 0$ at the leads. For $\Delta\mathbf{B} = 0$, the eigenvectors are

$$\sin(m_z \pi z / L_z) \cos(m_x \pi x / L_x) \cos(m_y \pi y / L_y),$$

where $m_z = 1, 2, \dots, \infty$, $m_{x,y} = 0, 1, 2, \dots, \infty$, and the eigenvalues are $\lambda = D(\pi/L_z)^2 \tilde{\lambda}_m$, where

$$\tilde{\lambda}_m = m_z^2 + m_x^2 (L_z^2/L_x^2) + m_y^2 (L_z^2/L_y^2) + \gamma - i\eta, \tag{3}$$

with $\gamma = (L_z/\pi L_{\text{in}})^2$, $L_{\text{in}} = (D\tau_{\text{in}})^{1/2}$ the inelastic dif-

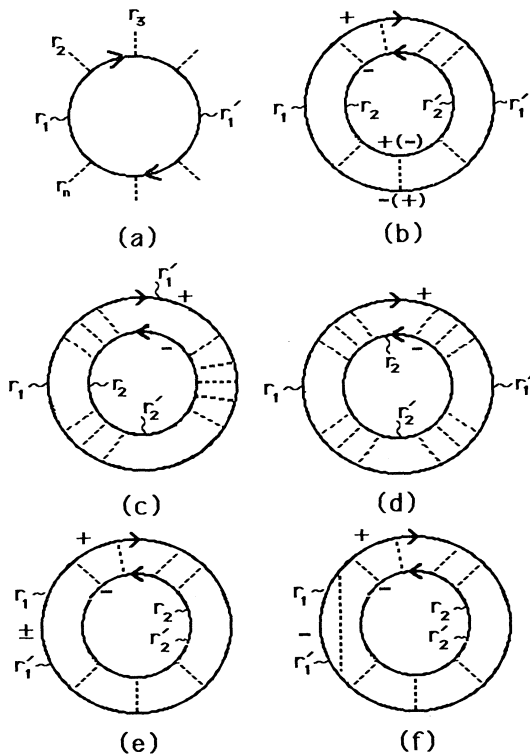


FIG. 1. (a) Unaveraged conductance. (b)–(f) Diagrams contributing to the correlation function; (e) and (f) are examples of a class of diagrams which cancel each other.

fusion length, and $\eta = \Delta E L_z^2 / \hbar \pi^2 D$. The evaluation of diagrams 1(c) and 1(d) is more complicated. In these diagrams there are single current vertices between diffusions which generate only a single derivative of P . Therefore, one must calculate matrix elements of the ϕ_μ , which do not cancel as they did in Fig. 1(b) by orthogonality.

So far we have restricted our discussion to the particle-hole channel. In the presence of normal im-

$$F(\Delta E, \Delta B = 0) = 2(4/\pi^2)^2 (F_{1(b)} + F_{1(c)} + F_{1(d)}), \quad (4)$$

where

$$F_{1(b)} = 2 \sum_{m_x, m_y=0} \sum_{m_z=1} [\text{Re}(\tilde{\lambda}_m^{-1})]^2, \quad (5)$$

$$F_{1(c)} = -8 \text{Re} \left[\sum_{m_x, m_y=0} \sum_{m_z=1} \sum_{n_z=2} \frac{(f_{mn})^2}{\tilde{\lambda}_m \tilde{\lambda}_n} \left(\frac{1}{\tilde{\lambda}_m} + \frac{1}{\tilde{\lambda}_n} \right) \right], \quad (6)$$

$$F_{1(d)} = 24 \text{Re} \left[\sum_{m_x, m_y=0} \sum_{m_z, p_z=1} \sum_{n_z, q_z=2} \frac{f_{mn} f_{np} f_{pq} f_{qm}}{\tilde{\lambda}_m \tilde{\lambda}_n \tilde{\lambda}_p \tilde{\lambda}_q} \right], \quad (7)$$

and $f_{mn} = 4m_z n_z / \pi (m_z^2 - n_z^2)$; the primes denote sums over even or odd integers only.

Equation (4) describes all the properties of the conductance fluctuations as a function of Fermi energy. First, the result for $\Delta E = 0$ ($\eta = 0$) and $L_{\text{in}}^{-1} = 0$ ($\gamma = 0$) gives us $\text{rms}(g)$, i.e., the typical size of the fluctuations at $T = 0$. We note again that the size of the conductor has totally canceled out, leaving only factors relating to its shape. In addition, the shape dependence is very weak since the lowest eigenvalue dominates the sums in Eq. (4) as long as $L_z \gg L_x, L_y$. Hence we find for a quasi-one-dimensional (1D) sample $\text{rms}(g) = 0.729$, for a 2D square $\text{rms}(g) = 0.862$ and for a 3D cube $\text{rms}(g) = 1.088$.

The second result obtained from Eq. (4) is the typical spacing between peaks and valleys in g as a function of E_F . This energy correlation range E_c is simply the half-width of $F(\Delta E)$. This is approximately determined by the condition $\eta = 1$, i.e., $E_c \approx \hbar \pi^2 D / L_z^2$, which is just the inverse time for the particle to diffuse across the sample in the current direction.⁸ In our scattering picture E_c may be interpreted as a resonance width which is much broader than the level spacing⁹; and then the conductance fluctuations have an exact analogy to "Ericson oscillations" of the scattering cross section in high-energy nuclear collisions,¹⁰ where the energy correlation range is also the resonance width.

The predictions of Eq. (4) may be tested by numerical simulations. In fact, earlier simulations² of the magnetic field fluctuations had provided the first indication of their very weak size dependence. The present simulations were performed by the same

purity scattering we can reverse the arrow in one of the loops in Figs. 1(b)–1(d) and obtain an equal contribution from the particle-particle channel. This contribution is suppressed by a magnetic field and by spin-orbit and spin-flip scattering. However, we emphasize that this is not equivalent to including the weak localization effects which usually arise from the particle-particle channel because we have not included these effects within a loop. Our final result for the correlation function is

method^{2,3} on a 2D nearest-neighbor tight-binding model with random site energies and with the same boundary conditions as above. The results, shown in Fig. 2, give excellent quantitative agreement with Eq. (4) with no free parameters. In particular, the inset shows that $\text{rms}(g)$ is indeed size independent, has the correct values in 1D and 2D, and is suppressed by a factor of $1/\sqrt{2}$ by a magnetic field. The results for $F(\Delta E)$ clearly show the increase in the half-width

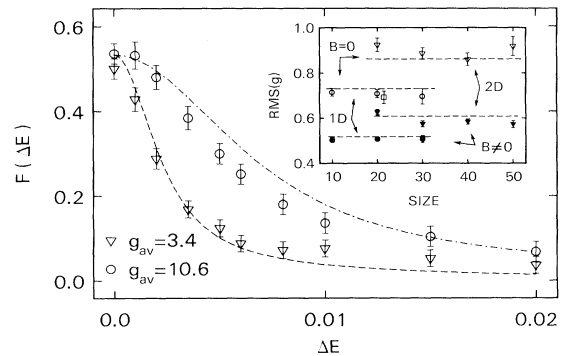


FIG. 2. Conductance correlation function vs ΔE (in units of the hopping matrix element) for two values of disorder ($\langle g \rangle = 3.4e^2/h$ and $10.6e^2/h$) for a 200×20 site wire. The circles and triangles are numerical results, and the dashed lines the results of Eq. (4) with no free parameters (E_c is estimated from the density of states per unit area of a 20×20 system with the same disorder). The inset plots $\text{rms}(g)$ (in units of e^2/h) vs width for a 2D square and a quasi-1D strip with length 10 times its width, with and without a magnetic field. The dashed lines are from Eq. (4).

with decreasing disorder, in good agreement with the relation $E_c = \hbar \pi^2 D / L_z^2$. Since $F(\Delta E)$ does decay as ΔE goes to infinity, as discussed above, we should be able to obtain the same value of $\text{rms}(g)$, not by ensemble averaging, but by summing over many energies E_i and $E_i + \Delta E$ for a given impurity configuration; this is verified by our simulation (such a calculation is shown as the square in the inset).

Now we consider $F(\Delta E = 0, \Delta B)$ which describes the structure in $g(B)$ already observed in small metal wires. Two important consequences immediately follow from the fact that only the field *difference* appears in the diagrams. First, the size of the oscillations in field $F(\Delta B = 0)$ is exactly as calculated above for the energy fluctuations in the presence of a field. Second, the oscillations should persist unchanged at least until $\omega_c \tau > 1$, the condition for the validity of the semiclassical approximation used above. This corresponds to a very high field in a metal and explains one of the most surprising features of the experiments. We can calculate the field correlation range, B_c , which determines the typical spacing of the fluctuations in B . To calculate $F(\Delta B)$ for arbitrary ΔB we must solve Eq. (2) with (choosing a gauge) $\Delta \mathbf{A} = e \Delta B y \hat{x}$. However, since our general solution for F is dominated by the lowest eigenvalue, B_c may be obtained simply from perturbation theory for this lowest eigenvalue, which gives

$$\begin{aligned} \tilde{\lambda}(m_z = 1, m_x = m_y = 0) &= 1 + \delta\lambda(\Delta B) \\ &\approx 1 + 1/12(L_z L_y e \Delta B / \pi)^2 \end{aligned}$$

for the quasi-1D case. B_c is determined by the condition $\delta\lambda(B_c) \approx 1$, which gives a result which may be expressed as $\Phi_c / \Phi_0 = \sqrt{3}$, where Φ_c is the change in magnetic flux through the area of the sample normal to the field, and $\Phi_0 = hc/e$ is the one-electron flux quantum (numerical calculations give a nonperturbative result¹¹ $\Phi_c / \Phi_0 \approx 2.4$). This area scaling of B_c had been obtained earlier in simulations,² and the predicted Φ_c agrees well with experiment.¹

The energy correlation range naturally sets the scale $kT_c \approx E_c$ for the crossover from a low- T regime, where the fluctuations are saturated at their zero-temperature amplitude, to a high-temperature regime in which the thermal effects begin to cause self-averaging. Interestingly enough, this crossover regime is accessible in small devices, typically occurring in the range 0.001–10 K. At higher T the fluctuations decrease as a slow power law of T . These predictions are consistent with the T dependence, amplitude, and saturation temperature observed experimentally.¹ Although here we report calculations on wires, we have extended the approach to treat metal rings and find¹¹ that the amplitude and behavior of the hc/e Aharonov-Bohm oscillations¹ are also described by a

theory of this type.

Our theory describes conductance fluctuations for weak disorder in 3D, and for weak disorder and samples shorter than the localization length in 1D and 2D; it does not apply to the strongly localized regime, where fluctuation phenomena have been extensively studied. The surprising result that the fluctuations are independent of sample size in the metallic regime may have been anticipated from the scaling theory of localization in two cases. Near the metal-insulator transition in three dimensions the conductance is scale independent and of order e^2/h . Then we may expect scale-independent conductance fluctuations, also of order e^2/h , since the fluctuations are known to be large in the localized regime. Also in the metallic regime in 2D the conductance is approximately scale independent, and since it is the only scaling variable, its fluctuations must also be scale independent. Indeed, a size-independent error bar from which $\text{rms}(g)$ can be determined was found in numerical tests of scaling theory.³ What is truly surprising is that the conductance fluctuations remain scale independent beyond these limiting situations.

One of us (P.A.L.) acknowledges the support of the National Science Foundation under Grant No. DMR-82-17956.

(a)Present address: Department of Physics, State University of New York at Stony Brook, Stony Brook, N.Y. 11794.

¹C. P. Umbach, S. Washburn, R. B. Laibowitz, and R. A. Webb, Phys. Rev. B **30**, 4048 (1984); R. A. Webb, S. Washburn, C. P. Umbach, and R. B. Laibowitz, Phys. Rev. Lett. **54**, 2696 (1985); S. Washburn, C. P. Umbach, R. B. Laibowitz, and R. A. Webb, Phys. Rev. B (to be published).

²A. D. Stone, Phys. Rev. Lett. **54**, 2692 (1985).

³D. S. Fisher and P. A. Lee, Phys. Rev. B **23**, 6851 (1981); P. A. Lee and D. S. Fisher, Phys. Rev. Lett. **47**, 882 (1981).

⁴E. Abrahams, P. W. Anderson, P. A. Lee, and T. V. Ramakrishnan, Phys. Rev. B **24**, 6783 (1981).

⁵P. F. Maldague, Phys. Rev. B **23**, 1719 (1981). Maldague evaluated the density response function, omitting a number of diagrams involving single impurity dressing across the density vertex, so that it is unclear whether the divergence he discussed is real.

⁶B. Altshuler, D. E. Khemelnitzskii, A. I. Larkin, and P. A. Lee, Phys. Rev. B **22**, 5142 (1980).

⁷B. L. Altshuler and A. G. Aronov, Pis'ma Zh. Eksp. Teor. Fiz. **33**, 515 (1981) [JETP Lett. **33**, 499 (1981)].

⁸A different heuristic argument implying $E_c \approx \hbar D / L^2$ has been given by Y. Imry; A. D. Stone and Y. Imry, unpublished.

⁹D. C. Licciardello and D. J. Thouless, Phys. Rev. Lett. **35**, 1475 (1976).

¹⁰T. Ericson and T. Mayer-Kuckuk, Annu. Rev. Nucl. Sci. **16**, 183 (1966).

¹¹A. D. Stone and P. A. Lee, unpublished.